Conference Proceedings

EuroSun 2016
Palma de Mallorca (Spain), 11-14 October 2016

Thermal Behavior of Photovoltaic-Thermal Hybrid Collector

Hiro Yoshida, Shigetoshi Daidouji, Kazutaka Itako and Naoto Hagino

Kanagawa Institute of Technology, Atsugi (Japan)

Abstract

Thermal behavior of the PV-T hybrid collector was examined using a simulator, where the PV cell is backed by the thermal collector. Heating effect of the PV cell (Joule heating by internal currents) was a main interest in this study. For the hybrid PV-T system, the thermal collector coefficient was prone to be larger in the case without external electric loads (open PV circuit) than in the case with the loads (closed PV circuit). Such trend was able to be explained analytically in terms of the internal heating phenomenon of PV. Results of field experiment by Sandnes and Rekstad (2002) show similar trend to the present one. The maximum heating power of the PV cell was confirmed to be equivalent to the maximum electric power of it. This result seems quite reasonable from the physical point of view. In the present PV-T configuration, the thermal collector coefficient drops significantly due to the shade effect of the PV cell placed in front of the thermal collector.

Keywords: *Photovoltaic cell, Joule heating, thermal collector, PV-T hybrid collector / simulator*

1. Introduction

The solar energy gives us an irreplaceable benefit. It is well known that a part of the energy is converted into electricity by the photovoltaic (PV) cells. The conversion rate of the cells will be practically 10-20 %. Regarding the remaining 80 % of the solar energy, our choice for now seems to be confined to using it as heat. Thus not only the electricity but the clever application of the heat is important. In many cases, the electricity and the heat are collected by the separate surfaces to each. It is natural that people come to an idea of collecting both electricity and heat by one common surface. Such device generally called photovoltaic and thermal (PV-T) hybrid collector. In the hybrid collector PV cell is often backed by the thermal collector.

The first publication on the PV-T hybrid model appeared about 40 years ago (Florschuetz, 1978). Up to now, many papers, mostly on the field experiments, have been published (for example, Chen and Riffat, 2011, Ito and Miura, 1993, Ibrahim, Othman, Ruslan, and Sopian, 2011, Sandnes and Rekstad, 2002). In one of the latest international conferences, EuroSun 2014 for example, discussions on the PV-T hybrid system was very active. To date, however, the performance of the PV-T hybrid system is not necessarily well understood (Yandri, Hagino, Itako, and Yoshida, 2012). Namely, the thermal coefficients of the hybrid collector showed different trend depending on whether the PV cell was connected to the external electric loads or not, where the electric loads are the household appliances such as TV, air-conditioner or lighting equipment (Yandri, Hagino, Itako, and Yoshida, 2012, Sandnes and Rekstad, 2002). It has been suggested that the internal heating (Joule heating) of the PV cell is supposed to affect the thermal characteristics of the hybrid collector (Yoshida, Daidouji, Itako, and Hagino, 2013). Based on the field experiment data, Sandnes and Rekstad (2002) also commented qualitatively on an excess heat generated by PV cell. Here, it might be interesting to ask what occurs in the PV cell under the irradiation when the cell is not connected to the loads (i.e. electricity generated is not properly taken out). In any case, direct observation of such phenomenon will be important for quantitative discussion.

In this study, aiming at further understanding about the thermal behavior of the PV-T hybrid system accompanying the PV internal heating, the authors tried to measure directly the heating effect of PV cell. For this purpose, a compact PV-T hybrid simulator was employed (Yandri, Hagino, Itako, and Yoshida, 2012).

doi:10.18086/eurosun.2016.08.17 Available at http://proceedings.ises.org

Through a series of experiments by the simulator, the behavior of the hybrid system was able to be examined more quantitatively.

2. Photovoltaic-thermal (PV-T) hybrid collector simulator

Figure 1 shows the schematic diagram of the PV-T simulator. It consists of the light source, the water supplying unit, and the PV cell (KIS Co.Ltd., model GT434, mono-crystalline type) backed by the thermal collector unit. The size of the PV cell is 1 mm thick (or less) and 378 x 349 mm^2 surface area. Side of the PV cell and the thermal collector were heat insulated by a 5 mm thick styrene foam sheet. In the precise measurement of the PV internal heating (section 4.4), the back surface of the thermal collector was covered by a 20 mm thick foam rubber. The heat conduction coefficients of the styrene foam and the foam rubber are 0.03 J/(mK) (JSME Data Book, 2009). In the preliminary experiment in section 4.1, the foam rubber was not set. The normal maximum output of the PV module is 13 W at 25 ^oC under the sun light. The 16 halogen bulbs (Ushio, model JDR110V40W LW/K) were used as the light source. The bulbs are arranged in a 4 x 4 matrix at equal intervals in the light source plane. The light source was placed underneath the PV-T collector surface facing downwards (Fig.1). Such arrangement (collector top - light source bottom) was adopted for the convenience of arranging cooling pipes and temperature sensors. Actually, due to this arrangement, the temperature field on the PV back surface was easily monitored by an infrared thermal view camera (Yoshida, 2010). The thermocouples for T_{in} and T_{out} (Fig.1) were attached through brass T-joints to a silicon rubber tube for cooling water. The thermocouple for T_{in} was placed at 1 m tube length from the inlet of the thermal collector and that for T_{out} was at 0.3 m from the outlet of the collector (Fig.A1 in Appendix). The outer and inner diameters of the silicon rubber tube were 11 mm and 5 mm, respectively. The light collecting surface is 0.38 m x 0.35 m area. The base structure of the simulator is the same as Yandri, et al (2012). In the present setup, a few improvements were added: 1) A center aperture was made at the center of the thermal collector unit to monitor PV temperature correctly (Fig.2); 2) The thermal collector unit was replaced by an aluminum plate with machined channel of cooling water (Yoshida,Daidouji, Itako, and Hagino, 2013). The imbedded channel is covered with a flat aluminum plate. A sheet of silicon rubber is placed between the channel and the aluminum plate (Fig.2). A flat surface is easy to manage heat transfer and heat insulation. Due to those modifications, temperatures of the PV unit and the thermal collector were able to be monitored

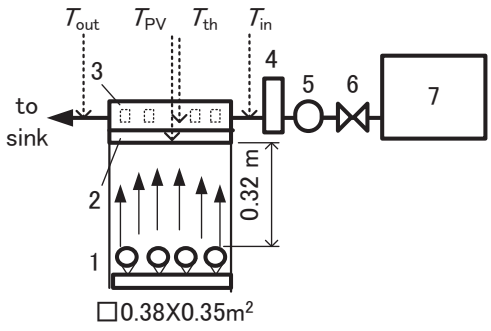

Figure 1 Schematic diagram of PV-T simulator: 1, light source (halogen light bulbs); 2, PV unit of 0.38 m x 0.35 m cross section; 3, thermal collector unit with cooling water channel; 4, flow meter; 5, circulating pump; 6, gate valve; 7, water tank. T_{in}, T_{out}, T_{th}, and T_{PV} are the temperatures of water at thermal collector inlet, outlet, center of the thermal collector and PV unit, respectively.

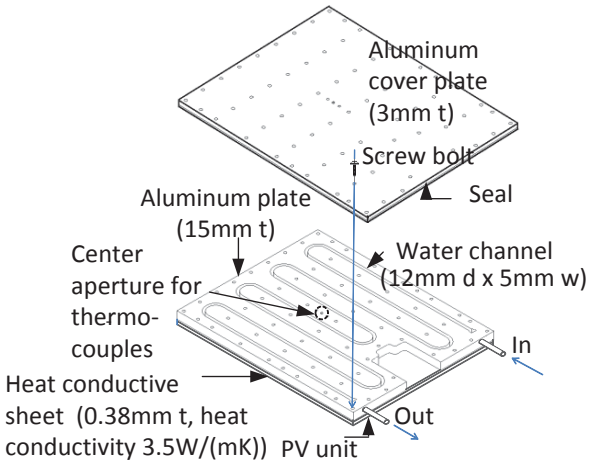

Figure 2 Aluminum plate thermal collector with cooling water channel. The center aperture was made for temperature measurement of PV and thermal collector.

simultaneously and correctly. Because the authors focused on the phenomena of internal heating of PV cell, effect of the light source position on the thermal collector performance was not examined.

Thermocouples of type T class 2 (CHINO, model 1STF013, precision measured by the authors was in the order of ∓0.2 ^{o}C) and a pyranometer (EKO INSTRUMENTS, model MS-42, internal resistance 500 Ω) were used for the temperature and the irradiation measurement, respectively. A float type flow meter (KOFLOC, RK1710-500/MIN) and a magnet pump for cooling water flow (SANSO, PMD-331B6K, 45W, 3L/min) were used. The temperature measurement was done when the simulator was under thermally steady state condition.

Regarding the convection heat transfer between the light source and the PV surface, the convection stream up to the PV surface was negligibly small, i.e. less than 0.3 m/s. As far as the light source and PV-T set (units 1 and 3 in Fig.1) was concerned, convection heat transfer was considered to be negligible. The effects of the room temperature and the convections on the piping tubes, attachments of thermocouples, and water tank (units 4 – 7 in Fig.1) will be concretely discussed later (section 4.4 and Appendix).

3. Thermal collector coefficient under additional heating in PV

In this section, we examine theoretically the thermal collector coefficient of the PV-T hybrid system for the case with an additional internal heating in the PV unit. It is quite reasonable to consider that the internal current in PV is prone to bring Joule heating effect. This effect is supposed to be maximized especially when the PV unit is not connected to the external electric loads. In the following, let us consider the thermal collector coefficient. The net thermal energy absorbed by the thermal collector unit, Q_{net}, is given as:

$$Q_{net} = Q_c - Q_{loss} \tag{1}$$

, where Q_c and Q_{loss} are the total thermal energy absorption and the total loss of the thermal collector unit, respectively. Referring to Huang and Du (1991), Q_c and Q_{loss} are defined as

$$Q_c = \alpha A I_0 \tag{2}$$

and

$$Q_{loss} = U\left(T_{out} - T_a\right) \tag{3}$$

In Eqs.(2) and (3), α, A, I_0, U, T_{out}, and T_{a} are, respectively, the non-dimensional effective solar absorptance, the collector surface area, the irradiation intensity incident upon the surface of the PV-T system, the coefficient of total heat loss, the temperature of water flowing out from the thermal collector unit, and the ambient temperature. In the present experiment, we took room temperature T_{room} as T_{a}. If there is an additional internal heating in the thermal collector, i.e. Joule heating in the PV unit, Eqs(2) and (3) can be modified as

$$Q_c^{'} = \alpha A\left(I_0 + \delta I\right) \tag{4}$$

$$Q_{loss}^{'} = U\left[\left(T_{out} + \delta T\right) - T_a\right] \tag{5}$$

, where δI and δT are the increments of the apparent irradiation and the water temperature at the thermal collector exit, respectively. Thus the thermal coefficient of the thermal collector, η'_{th}, under the additional heating is given as

$$\eta_{th}^{'} = \left(Q_c^{'} - Q_{loss}^{'}\right)/\left(AI_0\right) = \alpha^{'} - U^{'}\left(T_{out} - T_a\right)/I_0 \tag{6}$$

, where a' and U' are

$$\alpha^{'} = \alpha\left(1 + \delta I / I_0\right) \tag{7}$$

$$U^{'} = U\left[1 + \delta T /\left(T_{out} - T_a\right)\right] \tag{8}$$

In Eq.(6), let us name the term $(T_{out}\text{-}T_a)/I_0$ the temperature parameter. On the other hand, the thermal coefficient without the internal heating, η_{th}, , is given as

$$\eta_{th} = (Q_c - Q_{loss})/(AI_0) = \alpha - U(T_{out} - T_a)/I_0 \quad (9)$$

Comparing Eqs.(7) and (8), we easily see that

$$\alpha' \geq \alpha \text{ and } U' \geq U \quad (10)$$

Relationship (10) suggests that, if we plot η_{th} as a function of the temperature parameter $(T_{out}\text{-}T_a)/I_0$, the thermal coefficient of PV-T collector with the internal heating tends to be higher than that without it. More specifically, the inclination of the coefficient curve is steeper for the case with internal heating than that without it. This analytical examination will be confirmed experimentally in section4.3.

4. Experimental results

4.1 Starting behavior and various coefficients of PV-T simulator (*preliminary experiment*)

In this section a rough image of the general performance of the PV-T simulator was examined. In the experiment, back surface of the thermal collector was not covered by the rubber sheet. Effect of the room temperature will be discussed precisely in section 4.4. The irradiation intensity, I_0, was kept 1000 W/m^2 constant at the center of the PV surface, which was set 0.32 m above the light source (Fig.1). Distribution of irradiation intensity on the PV surface was measured by the pyranometer. On the surface, the irradiation was the largest at the center and smaller in peripheral area. The difference was less than 10 % (Takahashi and Nishiwaki, 2012).

Figure 3 shows temperature traces of PV unit for various cooling water flow rates, i.e. 100 – 600 cc/min. For those flow rates, the PV-T simulator reaches steady condition within an hour. After the steady condition, the temperature fluctuations around the mean value were less than ∓3 % for the flow rates of 100 cc/min and 200 cc/min, ∓6 % for 400 cc/min, and ∓10 % for 600 cc/min. The transition time of the present simulator is longer than that of the previous one (Yandri, Hagino, Itako, and Yoshida, 2012). However, as far as the steady state behavior is concerned, this is not the essential obstacle in the present study. To investigate non-steady behavior of the PV-T system, precise adjustment of the heat capacity of the collector will be necessary.

The PV power generation coefficient η_{PV} and the thermal collector coefficient η_{th} are compared in Fig.4, where η_{total} is the sum of them. The irradiation intensity was the same as the case of Fig.3, i.e. I_0=1000 W/m^2. In Fig.4, the coefficients at various PV temperatures 30.9, 32.7, 33.6, and 38.2 ^{o}C were obtained under the flow rates of 600, 400, 200, and 100cc/min, respectively. The higher flow rate tends to cause the lower PV temperature. In this figure, η_{PV} is about 0.05 for the temperatures considered and η_{th} ranges 0.4 to 0.55. As a result the total coefficient was around 0.5 – 0.6. It is clear that η_{th} is prevailing over η_{PV}. Although results are

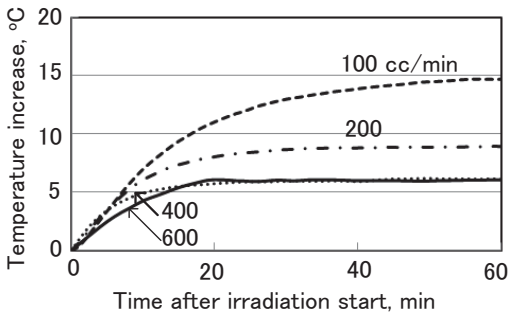

Figure 3 TempErature increase of PV unit after the irradiation start for various cooling water flow rate. Irradiation intensity is 1000 W/m^2.

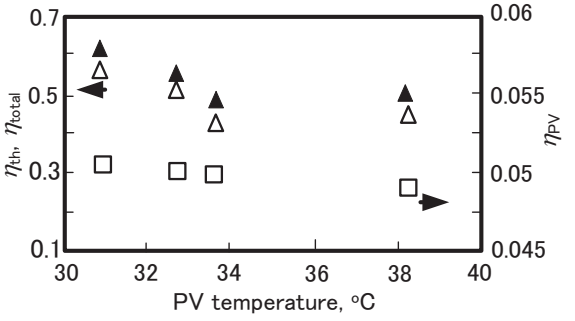

Figure 4 η_{PV}, η_{th}, and η_{total} vs PV temperature. Coefficients η_{PV}, η_{th}, and η_{TotaL} are designated by the symbols of open square, open triangle, and closed triangle, respectively. Irradiation intensity is 1000 W/m^2.

not shown here, our another experiment without PV cell in front of the thermal collector showed that η_{th} was above 80 % under the same flow rates and the irradiation conditions. Thus, in the present PV-T configuration, the thermal collector coefficient with PV cell dropped by roughly 40 % due to the shade effect of PV cell. This result seems quite understandable. The shading effect of the hybrid system is significant subject in future.

4.2. Internal (Joule) heating of PV cell

Hereafter, the open PV circuit and the closed PV circuit mean that the PV is connected to and not connected to the proper outside electric loads, respectively. Table 1 gives the measured data which are plotted in Figs.5 and 6. The irradiation intensity was set I_0=1000 W/m^2 constant as hitherto. Thus the actual irradiation input to the PV cell is 1000 W/m^2 x 0.378 m x 0.349 m = 132 W. The background temperature at each experiment was equal to the room temperature of the day. As can be read in Table 1, the temperature increase (T_{out}-T_{in}) for the open PV is larger than that for the closed PV by 0.2 ^{o}C - 1.2 ^{o}C for the flow rates considered. Those temperature increases are compared in Fig.5. As can be seen in this figure, the temperature increment in the open PV is distinguishable within the present experimental precision. At this stage, however, we can merely say that the Joule heating of PV may be detected. Amount of the Joule heating and effect of the room temperature will be discussed and handled more quantitatively in section 4.4.

Table 1 Data of PV open and closed, I_0=1000W/m^2

PV open

Flow rate	T_{PV}	T_{th}	T_{PV}-T_{th}	T_{in}	T_{out}	T_{out}-T_{in}	T_{room}	Power	$(T_{out}-T_{room})/I_0$	η_{th}
cc/min	^{o}C	^{o}C	^{o}C	^{o}C	^{o}C	^{o}C	^{o}C	W	^{o}C/(Wm^2)	
100	37.5	33.5	4.0	25.9	35.2	9.3	26.7	0	0.0085	0.49
200	31.1	27.0	4.1	22.9	28.2	5.3	24.2	0	0.004	0.55
400	29.9	26.0	3.9	23.9	26.7	2.8	23.2	0	0.0035	0.59
600	30.8	26.9	3.9	25.4	27.5	2.1	25.5	0	0.002	0.66

PV closed

Flow rate	T_{PV}	T_{th}	T_{PV}-T_{th}	T_{in}	T_{out}	T_{out}-T_{in}	T_{room}	Power	$(T_{out}-T_{room})/I_0$	η_{th}
cc/min	^{o}C	^{o}C	^{o}C	^{o}C	^{o}C	^{o}C	^{o}C	W	^{o}C/(Wm^2)	
100	38.2	34.5	3.7	27.5	36	8.5	28.2	6.52	0.0078	0.44
200	33.6	29.9	3.7	26.8	30.9	4.1	26.4	6.61	0.0045	0.43
400	32.7	29.0	3.8	27.3	29.7	2.4	25.8	6.61	0.0039	0.50
600	30.9	27.2	3.7	26.2	28	1.9	25.5	6.71	0.0025	0.57

Influence of the heat transfer between the simulator and the ambient air is considered as follows: The PV cell is irradiated in front surface. It transfers the heat to the ambient air in the room through the side surface and to the thermal collector through the back surface. If the coefficients of the heat transfer among PV, the ambient air, and thermal collector are the same in each experiment, it is reasonable to consider that the magnitudes of the heat releases from PV unit to the room and to the thermal collector must be proportional to the temperature differences i.e. (T_{PV}-T_{room}) and (T_{PV}-T_{th}). Thus amount of heat leaving from the side and the back surfaces of the PV unit can be estimated by A_s(T_{PV}-T_{room}) and A_b(T_{PV}-T_{room}), respectively, where A_s is the area of the side surface (1 mm thick x 2 x (378+349) mm periphery) and A_b is that of the back surface (378 mm wide x 349 mm height) of the PV unit. Using the data in Table 1, ratio of A_s(T_{PV}-T_{room}) and A_b(T_{PV}-T_{room}) was calculated as 0.02 – 0.03. That is, the heat release from the side surface of the PV unit is negligible compared to that from the back surface. The heat leaving from the thermal collector to the room is estimated by using the thermal property and geometry of the heat shield (section 2) and the temperature differences. Based on the above discussion and the data in Table 1, the heat loss from the back surface was calculated as 1 – 4 % of the thermal output, which was calculated by (mass flow rate) x (specific heat) x (measured T_{out}-T_{in}). On the other hand, the excess heat (difference of thermal outputs between open and closed PV cases) was 9 – 29 % of the thermal output in each experiment. Possibly, this result suggests that the internal (Joule) heating effect of PV might be maximized when it is not connected to the external electric loads.

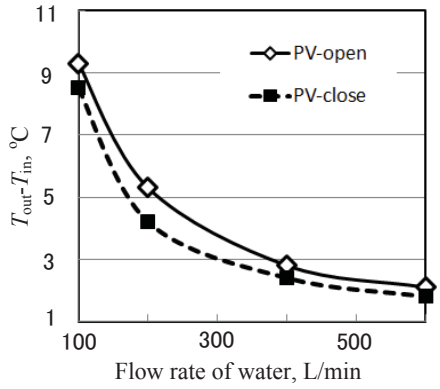

Figure 5 Temperature increase due to the internal heating of PV.

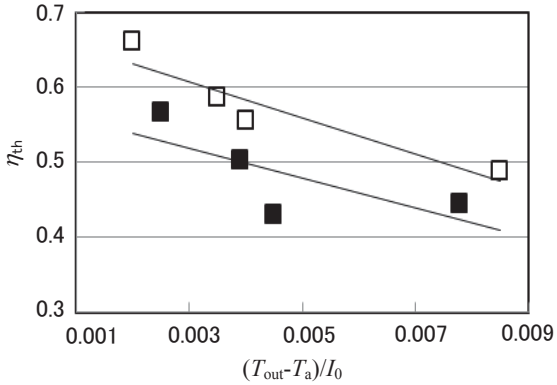

Figure 6 Thermal collector coefficient vs temperature parameter. Open and closed symbols indicate the cases of open and closed PV circuit, respectively.

The convection heat transfers were neglected and not taken into account in the present discussion. Effect of the room temperature and heat transfers including the convections will be discussed statistically in section 4.4 and Appendix.

In the case of the closed PV, the electric resistance of the circuit was controlled by the MPPT (Maximum Power Point Tracking) algorism (Itako, 2013) to generate maximum power output for various irradiation intensities. This algorism has been commonly applied already in the ordinary PV generation system.

4.3 Thermal collector coefficient with/without internal (Joule) heating of PV

The thermal coefficients of the open and the closed PV circuits are shown in Fig.6. As was forecasted in section 3, the coefficient of the open circuit is larger than that of the closed one. The regression lines in Fig.6 are: for the open circuit

$$\eta_{th} = 0.68 - 24(T_{out} - T_a)/I_0 \qquad (11)$$

, and for the closed circuit

$$\eta_{th} = 0.58 - 20(T_{out} - T_a)/I_0 \qquad (12)$$

In Eqs.(11) and (12), the ambient temperature T_a means the room temperature T_{room} in this study. Those equations indicate that $\alpha' = 0.68$, $U' = 24$ and $\alpha = 0.58$, $U = 20$, thus $\alpha' > \alpha$ and $U' > U$. This result is just the same as what suggested by Eq.(10). We can confirm that the experimental results by Sandness and Rekstad (2002) (Fig.5 in their paper) show the similar trend to the present results shown in Fig.6. Considering the Joule heating effect of the PV cell, we understand the reason of the trend of the thermal collector coefficient.

4.4 Joule heating and electricity output

In this section we examine the relationship between the thermal output of the PV cell when it is not connected to the outside electric loads (open PV) and the electric power output of it when it is properly connected to the loads (closed PV). To evaluate more correctly the heat generation by PV itself, influence of the room temperature on T_{in} and T_{out} (Fig.1) must be minimized. For this purpose the heat insulation of the thermal collector was improved: the back side of the thermal collector placed behind the PV cell was heat shielded by a foam rubber (section 2). Silicon rubber tubes connecting the inlet and the outlet of the thermal collector (Fig.A1) were left as they were. Three irradiation intensities of 800, 1000, and 1100 W/m^2 were chosen as I_0. At each irradiation the temperatures measured at least five times. The volume flow rate of cooling water was kept 200cc/min constant for each experiment. In Table 2 and 3 are given the measured raw temperatures and the modified temperature difference ($T'_{in} - T'_{out}$), where the effect of the room temperature was minimized. The procedure of calculation of the modified temperatures and the minimization is given in Appendix.

The data in Tables 2 and 3 are plotted in Figs.7 and 8. In Fig.7 are compared the raw temperature differences $\Delta T = (T_{out} - T_{in})_{open} - (T_{out} - T_{in})_{closed}$ and the corresponding modified temperature differences $\Delta T' = (T'_{out} - T'_{in})_{open} - (T'_{out} - T'_{in})_{closed}$. The suffixes "open" and "closed" indicate temperature differences under the open and the closed PV circuits, respectively. In the plot of ΔT and $\Delta T'$, the 1-σ (a standard deviation) error bars are superimposed. We can see in Fig.7 that both the raw ΔT (closed squares) and the modified $\Delta T'$ (open squares) tend to be positive. In the modified $\Delta T'$, a much clear dependency on I_0 can be seen. Those results indicate that the PV appreciably generates heat when it is not connected to the external electric loads. Figure 8 compares the thermal output of PV under unconnected circuit and the corresponding maximum electric power output under connected circuit. Within the present measurement precision, we can say that internal current of PV generates an appreciable amount of heat when it is not connected to the external electric loads. In other words, the maximum thermal output of unconnected PV is almost the same order of magnitude as the maximum electric power output of it under the same irradiation condition.

Table 2 Experimental data, reduced temperatures and thermal output for open PV circuit under 200 cc/min flow rate

I_0, W/m^2	T_{room}, °C	T_{PV}, °C	T_{in}, °C	T_{out}, °C	T_{out}-T_{in}, °C	$P_{th\text{-}o}$, W	T'_{out}-T'_{in}, °C	$P'_{th\text{-}o}$, W
800(1)	25.4	32.8	24.0	29.4	5.4	76.0	5.4	75.5
800(2)	23.4	31.8	23.3	28.3	5.0	69.3	5.2	72.7
800(3)	23.3	30.8	21.9	27.1	5.2	72.5	5.2	72.1
800(4)	22.3	30.3	21.6	26.9	5.2	73.2	5.3	74.9
800(5)	19.8	27.5	18.8	24.2	5.5	76.6	5.5	77.3
1000(1)	25.6	35.1	24.4	31.0	6.7	93.2	6.7	94.2
1000(2)	24.9	34.3	23.7	30.1	6.4	90.2	6.5	91.0
1000(3)	24.1	33.6	23.3	29.3	6.1	85.3	6.2	87.0
1000(4)	20.8	33.2	23.4	29.2	5.7	79.9	6.6	92.2
1000(5)	21.8	31.3	20.7	27.2	6.4	90.2	6.5	91.4
1100(1)	25.1	35.7	24.3	31.2	7.0	97.4	7.1	99.8
1100(2)	26.7	36.6	24.8	31.9	7.1	99.3	7.0	98.6
1100(3)	24.5	33.7	22.1	29.2	7.1	99.7	7.0	97.4
1100(4)	21.5	32.7	21.6	28.4	6.8	94.8	7.1	99.9
1100(5)	25.3	37.6	27.2	33.3	6.1	85.4	6.8	95.6

Table 3 Experimental data, reduced temperature and difference of thermal outputs for closed PV circuit under 200cc/min flow rate

I_0, W/m^2	T_{room}, °C	T_{PV}, °C	T_{in}, °C	T_{out}, °C	T_{out}-T_{in}, °C	$P_{th\text{-}c}$, W	T'_{out}-T'_{in}, °C	$P'_{th\text{-}c}$, W	P_{el}, W	$P'_{th\text{-}o}$-$P'_{th\text{-}c}$
800(1)	25.5	32.5	24.4	29.3	4.9	68.0	4.9	68.0	5.33	8.0
800(2)	23.3	31.3	23.6	28.1	4.5	63.3	4.8	67.2	5.28	6.0
800(3)	23.6	31.1	23.0	27.6	4.6	64.4	4.7	65.6	4.98	8.1
800(4)	22.7	29.6	21.6	26.3	4.6	64.8	4.6	64.9	5.24	8.4
800(5)	19.5	26.8	18.6	23.6	5.0	70.3	5.1	71.1	5.27	6.3
1000(1)	26.8	34.7	24.6	30.8	6.2	87.2	6.0	84.7	7.22	6.0
1000(2)	24.0	33.0	23.1	29.0	6.0	83.9	6.1	85.2	7.09	6.3
1000(3)	24.0	32.8	23.3	28.8	5.5	77.3	5.7	79.2	7.05	8.0
1000(4)	20.7	30.8	21.3	26.9	5.7	79.5	6.1	85.3	7.09	0.4
1000(5)	22.6	30.6	20.5	26.5	6.0	84.0	5.8	81.9	7.18	6.2
1100(1)	25.0	34.4	23.7	30.0	6.3	88.2	6.3	88.6	8.11	9.2
1100(2)	26.6	36.1	25.4	31.8	6.3	88.5	6.4	89.3	7.99	10.8
1100(3)	23.7	31.0	20.0	26.5	6.5	91.3	6.0	84.6	7.89	8.4
1100(4)	21.5	31.9	21.6	27.7	6.2	86.2	6.5	90.8	7.92	8.5
1100(5)	25.9	36.3	26.8	32.4	5.6	78.5	6.1	85.2	7.83	6.9

.

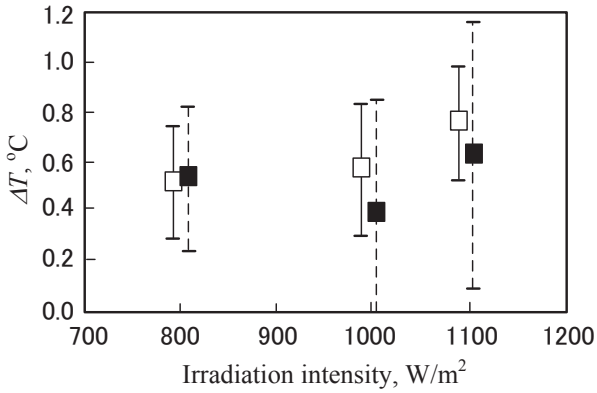

Figure 7 Temperature difference ΔT between (T_{out}-T_{in}) for the open and the closed PV circuits vs the irradiation intensity. ΔT =(T_{out}-T_{in})$_{open\ PV}$-(T_{out}-T_{in})$_{closed\ PV}$. Open and closed square symbols denote the results with and without modification of the room temperature, respectively. 1-σ error bars are superimposed on the both ΔT results.

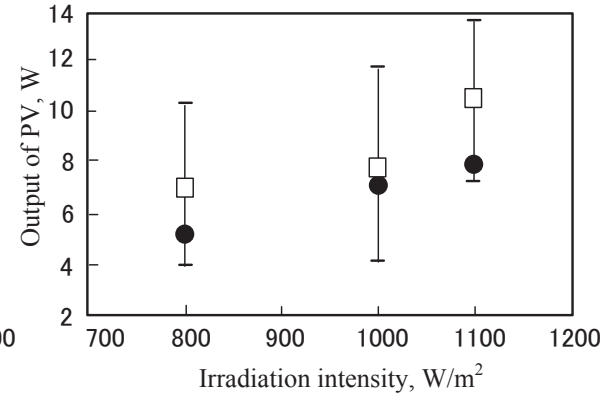

Figure 8 Thermal and electric Output Of P vs the irradiation intensity. Open square and closed circle symbols denote thermal output for open PV circuit and electric output of PV for closed PV circuit, respectively. 1-σ error bars is superimposed on the thermal output.

5. Concluding remarks

The thermal behavior of the photovoltaic-thermal (PV-T) hybrid collector was examined using a simulator, especially focusing on the cases when PV cell was connected to (closed) and not connected to (open) external electric loads. The main results are summarized as follows:

1) For the hybrid PV-T system: it was confirmed that the thermal collector coefficient was prone to be larger in the case without the external electric loads (open PV) than the case with them (closed PV). Such trend was well explained in terms of the internal heating phenomenon (Joule heating) of the PV cell. Field experiment by Sandnes and Rekstad (2002) show the similar trend to the present one. In the present PV-T configuration, thermal collector coefficient drops significantly due to the shade effect of the PV cell. Overcoming such defect and improving total coefficient may be an important subject in future study.

2) For the Joule heating of the PV cell: the heating phenomenon was directly observed by the simulator. The maximum heating power of the PV cell was confirmed to be equivalent to the maximum electric power of it. This result seems quite reasonable from the physical point of view.

In the last the authors would like to express their sincerer thanks to Messes E.Yandri, N.Nishiwaki, K.Takahashi, and S.Ono for their help in the experiments. The present study was performed under the special grant of Kanagawa Institute of Technology.

6. References

Chen,H. and Riffat,S.B., Development of photovoltaic thermal technology in recent years: a review, International Journal of Low-Carbon Technologies, Vol.6 (2011), pp.1-13.

EuroSun 2014, International Conference on Solar Energy and Buildings was held in September 16-19, 2014, in Aix-le-Bains, France. In addition to the session on the PV-T hybrid system, some commercial products of PV-T system were displayed.

Florschuetz L.W., Extension of the Hottel-Whillier model to the analysis of combined Photovoltaic/thermal Flat-Plate collectors, Solar Energy, Vol.22, pp.361-366, 1978.

Huang, B. J. and Du, S. C., A performance test method of solar thermosyphon systems, Transactions of the ASME, Journal of Solar Energy Engineering, Vol.113 (1991), pp.172-179.

Ibrahim, A., Othman, M.,Y., Ruslan, M.H., Mat, S., and Sopian, K., Recent advances in flat plate photovoltaic/thermal (PV/T) solar collectors, Renewable and Sustainable Energy Reviews, Vol.15, pp.325-365, 2011.

Imada, H., Hagino, N., and Yoshida, H., Field experiment of solar thermosyphon, Transactions of the JSME B, Vol.79 (2013), No.801, pp.809-813 (in Japanese).

Itako, K., New I-V Characteristics Scan-Type MPPT Control Method for PV Generation System" Journal of Technology Innovations in Renewable Energy (USA),Vol.1, (2013), No.2,pp.87-91.

Ito, S. and Miura, N., Solar air collector using photovoltaic modulus as the cover, Proceedings of ISES Solar World Congress, Budapest, Vol.3 (1993), pp.271-276.

JSME Data Book: Heat Transfer, 5th edition (2009), p.290, Maruzen, Tokyo (in Japanese).

Peuser, F. A., Remmers, K.-H., and Schnauss, M., Solar Thermal Systems (2002), Solarpraxis Berlin.

Sandnes B., and Rekstad J., A photovoltaic/thermal collector with a polymer absorber plate, experimental study and analytical model, Solar Energy, Vol. 72 (2002), No.1, pp. 63-73.

Takahashi,K. and Nishiwaki,N., PV-T simulator, Kanagawa Institute of Technology graduate thesis, 12YSD03 (2012) (in Japanese).

Tamaura, Y., et al, Solar Energy – front of effective utilization – (2008), NTS (in Japanese).

Yandri, E., Hagino, N., Itako, K., Yoshida, H., Basic characteristics of a compact PV/T simulator, ASME ICONE20-POWER2012 (2012), Paper No.54216.

Yoshida, H., Annual Report of 2010 (No. 4), Solar Energy System R & D Center, Kanagawa Institute of Technology, pp.7-11 (in Japanese).

Yoshida,H., Daidouji,S., Itako,K., Hagino,N., Characteristics of photovoltaic-thermal collector tested by a simulator, JSME, 23rd Kankyo Kogaku Symposium (2013), No.13-15, 405, pp.286-287 (in Japanese).

Appendix

1. Effect of room temperature and heat losses

We consider in section 4.4 that effect of the room temperature on T_{out} - T_{in} mainly originated from the heat exchange through the silicon rubber tubes of 0.3 m long and 1 m long. Shorter one is for the outlet and the longer one for the inlet of the thermal collector, respectively. The situation considered is depicted in Fig.A. Heat exchanges through the other units except those tubes are considered to be negligible. The thermal entrance region (length) of the tubes was estimated to be over 1.5 m in the present experimental condition. For a reference, Reynolds number and Prandtl number were ≈ 900 - 1100 and ≈ 5 - 7, respectively. Exact analytical approach for deciding the temperatures without the room temperature effect seemed difficult. Thus a statistical but mathematically reasonable method of data analysis was adopted in the following.

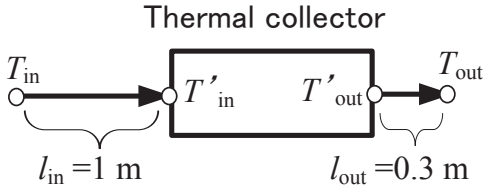

Figure A1 Silicon rubber tubes connected to the inlet and the outlet of the thermal collector. The main heat exchange between the simulator and the ambient is supposed to occur through the tubes.

Based on the observed data, we assume $T_{room} < T'_{in} < T_{out} < T'_{out}$ simply as an aid in the following procedure. The temperatures T_{room}, T_{in}, and T_{out} are the measured ones and T'_{in}, and T'_{out} are the modified ones, in which the room temperature effect is minimized. It is obvious that this

inequality assumption on the temperatures does not violate the validity of the present approach.

1. Heat transfer between the silicon tubes and the ambient

Let the heat transfers through the tube l_{in} and l_{out} be Q_{in} and Q_{out}, respectively. It seems reasonable to assume that those heat transfers are given as Eqs. (A1) and (A2):

$$Q_{in} = A_{in} h_{in} \left[\left(\frac{T_{in} + T'_{in}}{2} \right) - T_{room} \right] \quad \text{(A1)}$$

$$Q_{out} = A_{out} h_{out} \left[\left(\frac{T_{out} + T'_{out}}{2} \right) - T_{room} \right] \quad \text{(A2)}$$

, where h_{in} and h_{out} are empirical coefficients of heat transfer evaluated statistically and A_{in} and A_{out} are the surface area of the tubes given as Eq. (A3).

$$A_{in} = l_{in} \pi d, \; A_{out} = l_{out} \pi d \quad \text{(A3)}$$

, where d is the outer diameter of the silicon tube. Using mass flow rate m and specific heat C of the cooling water, Eqs.(A1) and (A2) are rewritten as

$$Q_{in} = mC\left(T_{in} - T'_{in}\right) \quad \text{(A4)}$$

$$Q_{out} = mC\left(T_{out} - T'_{out}\right) \quad \text{(A5)}$$

From Eqs. (A1), (A2), (A4), and (A5), modified temperatures T'_{in}, and T'_{out} are decided as follows,

$$T'_{in} = \frac{-\left(\frac{1}{2} - \frac{mC}{ak} \right) T_{in} + T_{room}}{\left(\frac{1}{2} + \frac{mC}{ak} \right)} \quad \text{(A6)}$$

$$T'_{out} = \frac{-\left(\frac{1}{2} + \frac{mC}{k} \right) T_{out} + T_{room}}{\left(\frac{1}{2} - \frac{mC}{k} \right)} \quad \text{(A7)}$$

, where a factor a is the ratio of the tube lengths $l_{in}/l_{out} \approx 3.3$ and a parameter k is given as $k = \pi d l_{out} h$, respectively. In Eqs.(A6) and (A7), we can easily confirm that $T'_{in} \rightarrow T_{in}$ and $T'_{out} \rightarrow T_{out}$ when $k \rightarrow 0$.

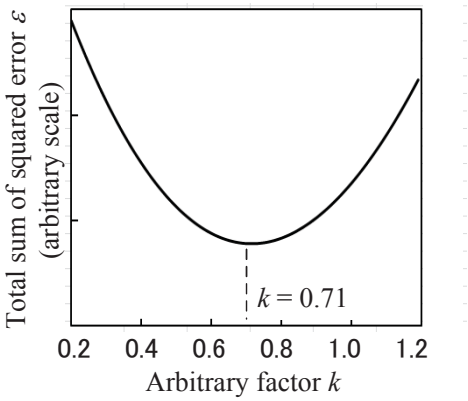

Figure A2 Total sum of squared errors vs k

2. Calculation of k and $T'_{out} - T'_{in}$

Using Eqs.(A6) and (A7), we can define the error in $T'_{out} - T'_{in}$ for experiments i and j done under the common irradiation condition. The error ε_{ij} and sum of squared ones ε are defined as

$$\varepsilon_{ij} = \left(T'_{out} - T'_{in}\right)_i - \left(T'_{out} - T'_{in}\right)_j \quad \text{(A8)}$$

$$\varepsilon = \sum_{i,j} \varepsilon_{ij}^2 \quad \text{(A9)}$$

The factor k was calculated so as to minimize ε. In Fig.A2 is plotted ε for all temperature data given in Table 2 and 3 as a function of k. As can be seen in this figure, we find the error is minimum at $k \approx 0.71$. Using the relationship $k = \pi d l_{out} h$, the corresponding heat transfer coefficient h is evaluated to be $\approx$ 70 W/(m^2 K). The temperatures $T'_{out} - T'_{in}$ in Table 2 and 3 are calculated by using Eqs. (A6) and (A7) with k = 0.71.

3. Symbols for quantities

Quantity	Symbol	Unit
Area	A	m^2
Specific heat	C	J kg^{-1} K^{-1}
Diameter of tube	d	M
Heat transfer coefficient	h	W m^{-2} K^{-1}
Irradiation intensity	I	W m^{-2}
A parameter (Appendix)	k	W K^{-1}
Length of tube (Appendix)	l	M
Mass flow rate	m	Kg s^{-1}
Heat flow rate	Q	W
Temperature	T	K
Coefficient of total heat loss	U	W K^{-1}
Effective absorptance	α	0
Difference	δ	0
Error (Appendix, Eq.(A8))	ε_{ij}	K
Error (Appendix, Eq.(A9))	ε	K^2
Efficiency	η	0

4. Subscripts

Quantity	Symbol
Ambient condition	*a*
Total energy	*c*
PV with electric loads	*closed*
Inlet condition	*in*
Loss	*loss*
Net energy	*net*
Outlet condition	*out*
PV without electric loads	*open*
Photovoltaic cell	*PV*
Thermal collector	*th*
Reference value	0

5. Superscripts

Quantity	Symbol
Relating additional heating or reduced, modified quantities	‘